Diagn Interv Radiol 2020; 26:87–94

ABDOMINAL IMAGING

ORIGINAL ARTICLE

Multiparametric MRI of rectal cancer—repeatability of quantitative data: a feasibility study

Bengi Gürses
Emre Altınmakas
Medine Böge
M. Serhat Aygün
Onur Bayram
Emre Balık

PURPOSE
In this study, we aimed to analyze the repeatability of quantitative multiparametric rectal magnetic resonance imaging (MRI) parameters with different measurement techniques.

METHODS
All examinations were performed with 3 T MRI system. In addition to routine sequences for rectal cancer imaging protocol, small field-of-view diffusion-weighted imaging and perfusion sequences were acquired in each patient. Apparent diffusion coefficient (ADC) was used for diffusion analysis and k_{trans} was used for perfusion analysis. Three different methods were used in measurement of these parameters; measurements were performed twice by one radiologist for intraobserver and separately by three radiologists for interobserver variability analysis. ADC was measured by the lowest value, the value at maximum wall thickness, and freehand techniques. K_{trans} was measured at the slice with maximum wall thickness, by freehand drawn region of interest (ROI), and at the dark red spot with maximum value.

RESULTS
A total of 30 patients with biopsy-proven rectal adenocarcinoma were included in the study. The mean values of the parameters measured by the first radiologist on the first and second measurements were as follows: mean lowest ADC, 721.31±147.18 mm^2/s and 718.96±135.71 mm^2/s; mean ADC value on the slice with maximum wall thickness, 829.90±144.24 mm^2/s and 829.48±149.23 mm^2/s; mean ADC value measured by freehand ROI on the slice with maximum wall thickness, 846.56±136.31 mm^2/s and 848.23±144.15 mm^2/s; mean k_{trans} value on the slice with maximum wall thickness, 0.219±0.080 and 0.214±0.074; mean k_{trans} by freehand ROI technique (including as much tumoral tissue as possible), 0.208±0.074 and 0.207±0.069; mean k_{trans} measured from the dark red foci, 0.308±0.109 and 0.311±0.105. Intraobserver agreement was very good among diffusion and perfusion parameters obtained with all three measurement techniques. Interobserver agreement was very good, except for one of the measurement techniques. As far as interobserver variability is considered, only ADC value measured on the slice with maximum wall thickness differed significantly.

CONCLUSION
Multiparametric MRI of rectum, using ADC as the diffusion and k_{trans} as the perfusion parameter is a repeatable technique. This technique may potentially be used in prediction and evaluation of neoadjuvant treatment response. New studies with larger patient groups are needed to validate the role of multiparametric MRI.

From the Departments of Radiology (B.G. ✉ *bgurses@kuh.ku.edu.tr*, E.A., M.B., M.S.A.) and General Surgery (O.B., E.B.), Koç University School of Medicine, İstanbul, Turkey.

Received 11 March 2019; revision requested 06 April 2019; last revision received 15 October 2019; accepted 22 October 2019.

Published online 13 January 2020.

DOI 10.5152/dir.2019.19127

Rectal cancer is the second most common form of cancer in females and third most common cancer in males, worldwide. Rectal cancer constitutes a significant clinical burden, with almost 40 000 new patients in the USA, in 2015 (1). Magnetic resonance imaging (MRI) has been the mainstay of local staging in patients with newly diagnosed rectal cancer. Overall, MRI has high sensitivity for initial local staging of the tumor, as far as "T" staging is considered. MRI has the potential to evaluate and predict circumferential resection margin (CRM), extramural venous invasion and extramural extension of the tumor, with high accuracy. In addition, studies have demonstrated that it is a reproducible technique with high specificity (92%) for predicting depth of invasion beyond muscularis propria (2, 3).

You may cite this article as: Gürses B, Altınmakas E, Böge M, Aygün MS, Bayram O, Balık E. Multiparametric MRI of rectal cancer—repeatability of quantitative data: a feasibility study. Diagn Interv Radiol 2020; 26:87–94.

Currently, neoadjuvant treatment consisting of chemo- and radiotherapy (CRT) is applied for rectal carcinomas in locally advanced stage. The role of neoadjuvant treatment has been established and is well known to reduce local recurrence and increase disease-free survival (4). MRI not only provides primary local staging for tumors except T1 and T2 stage, it also has a role in the prediction of response to neoadjuvant therapy. Accurate evaluation of treatment response and detection of complete response have crucial value in the treatment strategy of this patient group. Approximately 15%–25% of patients have complete response to neoadjuvant treatment, while 25%–45% have poor response and the remaining patients have partial response (5). The sensitivity of MRI in terms of response evaluation is less compared with its sensitivity for initial staging. The reason is limited capability of conventional MRI sequences to discriminate between tumoral tissue and treatment induced inflammation, edema, and fibrosis. Conventional MRI sequences, even with optimal technique, have limited value in detection of complete response (6), although there are some promising data about diffusion-weighted imaging (DWI) (7). PET/CT may also be used to detect response to treatment, but it is not an ideal modality and has well-known limitations, especially in mucinous tumors with low FDG affinity (8). There is great effort to perform initial staging and, more importantly, detect treatment response noninvasively and accurately. Besides, there is also great interest to noninvasively predict which patients will have good response or will not respond at all to neoadjuvant treatment, at the beginning or initial stages of treatment, to avoid treatment-related morbidity (5).

Main points

- Diffusion parameters derived from small FOV DWI have very good intraobserver agreement.
- Diffusion parameters derived from small FOV DWI have very good interobserver agreement, except for one of the measurement techniques.
- Multiparametric MRI of the rectum is a feasible technique with good repeatability.
- K_{trans} parameter derived from perfusion imaging has good inter- and intraobserver agreement.

Multiparametric MRI of rectum includes DWI and perfusion techniques, in addition to routine sequences. This technique has not yet been incorporated into routine clinical practice. It is focused on tumor biology and is relatively new; there are only limited number of articles about this topic in the literature (4, 9, 10, 11, 12, 13). In 2016, according to the results of European Society of Gastrointestinal and Abdominal Radiology (ESGAR) consensus meeting, DWI technique managed to improve results for differentiating between complete and partial response. On the other hand, the authors concluded that the results of DWI should be evaluated in a qualitative manner since there is no current role for quantification of ADC and validated thresholds. As far as perfusion-weighted MRI is concerned, the panel reached full consensus that this modality should be accepted as a research tool currently and not adopted routinely (14, 15).

DWI relies on thermally driven random motion of water molecules in tissues. In the presence of cancerous tissue, where there is increased cellularity and change in cellular membrane integrity, diffusion restriction occurs, which can be shown with DWI. The use of DWI technique has an incremental course in both primary and treatment response evaluation for rectal cancer imaging (4, 9–11).

Perfusion MRI relies on the dynamic assessment of kinetics of contrast uptake. A T1-weighted sequence with high temporal resolution is used for this technique. After acquisition, the data can be evaluated with different pharmacokinetic models (e.g., Tofts, Tofts and Kermode, and Brix et al. models). In our institution, the TWIST (time resolved MRA – echo-shared, high spatial and temporal resolution, time resolved sequences with interleaved stochastic trajectories) sequence was used, with a temporal resolution of 2.9 s. The k_{trans} value was obtained using the Tofts model. K_{trans} is a measure of capillary permeability, which describes the transendothelial transport of the contrast medium (16, 17).

There are only a few studies dealing with the feasibility of multiparametric rectal MRI (9, 18–20. In this study, we analyzed the feasibility of multiparametric MRI of the rectum in patients with rectal carcinoma. Small field-of-view (FOV) diffusion sequence is used for DWI, different from previous publications. Different measurement techniques were performed for both diffusion and perfusion sequences and intra- and interobserver variability was determined. We aimed to set up the multiparametric MRI technique and detect the repeatability of the measurements in patients with newly diagnosed rectal cancer.

Methods

Patient group

The multiparametric MRI technique for rectal cancer has been initiated in our department in January 2017. A total of 30 patients (19 male, 11 female) with newly diagnosed rectal adenocarcinoma with endoscopy and biopsy, who underwent MRI for local staging between January 2017 and March 2019 were included retrospectively, in this study. The mean age of the patients was 58.9 years (age range, 32–80 years). All patients had undergone endoscopic biopsy and proven to be rectal adenocarcinoma. Informed consent was obtained from each patient prior to the MRI examination. The study was approved by the local ethics committee (2018.330.IRB2.056)

MRI technique

All the MRI examinations were performed with a 3 T system (Skyra, Siemens), using 18-channel pelvic phased-array coil. In all patients, approximately 5 minutes before the MRI examination, an antiperistaltic agent was administered by intravenous route to decrease peristaltic movement-related artifacts. Initially, axial T1-weighted turbo spin echo (TSE) and fat saturated T2-weighted sequences were acquired including the whole pelvis. Afterwards, high-resolution (HR) T2-weighted TSE was acquired at the sagittal plane. On sagittal T2-weighted images, the pathological segment was identified by the abdominal radiologist during MRI acquisition, and the plane of the axial and coronal oblique T2-weighted images were planned accordingly. Great care was taken to adjust the axial oblique image perpendicular and the coronal oblique image plane parallel to the tumoral segment. The image parameters of HR T2-weighted sequences were: TR, 5600 ms; TE , 117 ms; slice thickness, 3 mm; flip angle, 155°; FOV, 200×200; matrix, 512×512. After routine imaging with rectum cancer protocol was completed, DWI sequence with small FOV technique (Zoom it DWI) was acquired including the pathological segment with an axial oblique angle identical to the axial oblique plane of HR T2 sequence. DWI parameters were as follows: TR, 5574 ms; TE, 80 ms; FA, 90°; FOV, 76×120; matrix, 58×98; *b* values, 50-400-

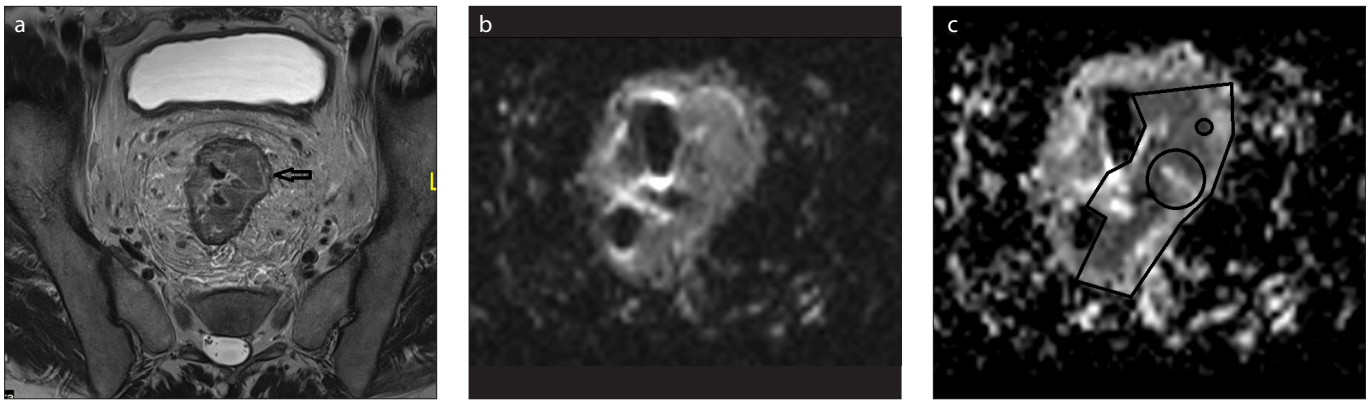

Figure 1. a–c. Axial oblique high-resolution T2-weighted TSE image **(a)** shows a midrectal tumor with diffuse wall thickening *(arrow)*. "Zoom it DWI" image **(b)** of the same slice and ADC map **(c)** are shown.

800 s/mm^2. Perfusion-weighted imaging was performed with TWIST sequence (TR, 4.8; TE, 1.9; FA, 12°; FOV, 260×260; matrix, 192×192; slice thickness, 3.5 mm; views per slice, 60; temporal resolution, 2.9 s) using intravenous gadolinium based agent (Dotarem, Guerbet) with an infusion rate of 2 mg/kg, followed by 40 mL of saline flush, injected at the identical rate. The contrast injection was performed with an automatic injector. The acquisition plane of perfusion sequence was set identical with the axial oblique HR T2 and axial oblique Zoom it DWI sequences. The dynamic sequence lasted for 5.25 minutes and a total of 59 phases are obtained.

Analysis of MRI data

Three radiologists with at least 6 years of experience in abdominal imaging (B.G., M.B., E.M.) evaluated the multiparametric MRI data, separately, for interobserver analysis. One of the radiologists with 14 years of experience in abdominal radiology (B.G.) performed all the measurements twice, for intraobserver analysis. Data analysis was carried out on a specialized workstation with dedicated software, provided by Siemens (Leonardo). Initially, each reader evaluated the conventional sequences and performed local staging of the tumoral segment and recorded. The length of the tumoral segment, maximum wall thickness were measured and recorded. The image position with maximum wall thickness was determined by each reader and recorded. Afterwards, analysis of DWI images were performed with apparent diffusion coefficient (ADC) measurements. For DWI analysis, two separate ADC measurements were done and the mean value was recorded. First measurement included the ADC value obtained where there is maximum wall thickening at the image position identical to T2-weighted HR image that has been recorded before. Second measurement included the ADC value obtained from the visually most hypointense foci on ADC map, to find out the most restricted area. Afterwards a third measurement was performed where freehand ROI was used to include as much tumoral tissue as possible where there is maximum wall thickening. ROI size and number of pixels were selected by each reader as to maximize ROI size, with the smallest ROI containing at least 8 pixels. Great care was taken to exclude any structure (e.g., vessel, lumen, mesorectal fat) outside the tumor during ROI placement. Axial oblique HR T2 TSE, Zoom it DWI and ADC map images of a patient is given in Fig. 1. Analysis of perfusion data was performed with tissue 4D software technique, provided by Siemens. The first ROI was inserted on the internal iliac artery for arterial input function. Afterwards, the volume of interest was selected as to include the tumoral segment. K_{trans} maps were then generated automatically by the help of the dedicated software using a two-compartment Toft model. Two separate k_{trans} measurements were performed with three different methods and their mean value was recorded. First, the ROI for k_{trans} value was inserted to the region where there is maximum wall thickening on T2-weighted HR image, similar to ADC measurement. Second, freehand ROI was performed to include as much tumor tissue as possible at the slice where there is maximum wall thickening on T2-weighted HR image. Afterwards, the ROI was inserted where the color coded map is dark red, to identify the k_{trans} value where there is highest deviation from normal perfusion parameters. The ROI sizes were determined by each reader to include as much pathological tissue as possible. The smallest ROI contained 8 pixels. ROI placements with three different measurement techniques on perfusion sequence is shown in Fig. 2. Since this is a repeatability study, K_{ep} values were not calculated, not to further increase the amount of data.

Statistical analysis

Since the number of patients in this retrospective study is limited with 30, nonparametric analysis was preferred. Wilcoxon test (paired sample) was used to compare two different measurements of the same observer. For comparison of measurements of the same observer, Bland Altman analysis was also performed. For the same patients, to compare the parameters measured by three different observers, Friedman ANOVA (paired sample) test was used. Bland Altman analysis was also performed for comparison of measurements of different observers. Graphics were created for Bland Altman analysis to find out if the point dispersions were appropriate. For all the statistical methods, significance value was accepted as α=0.05. Statistical analysis was performed using SPSS (IBM) 20.0 and NCSS 19.02.

Results

Each reader evaluated the tumoral tissue in all 30 patients as pathological wall thickening. None of the lesions were in the form of a mass. All readers staged 28 patients as having T3 and the remaining 2 patients as having T2 disease.

There were a total of 8 parameters measured by each radiologist: wall thickness, length of involved segment, lowest ADC

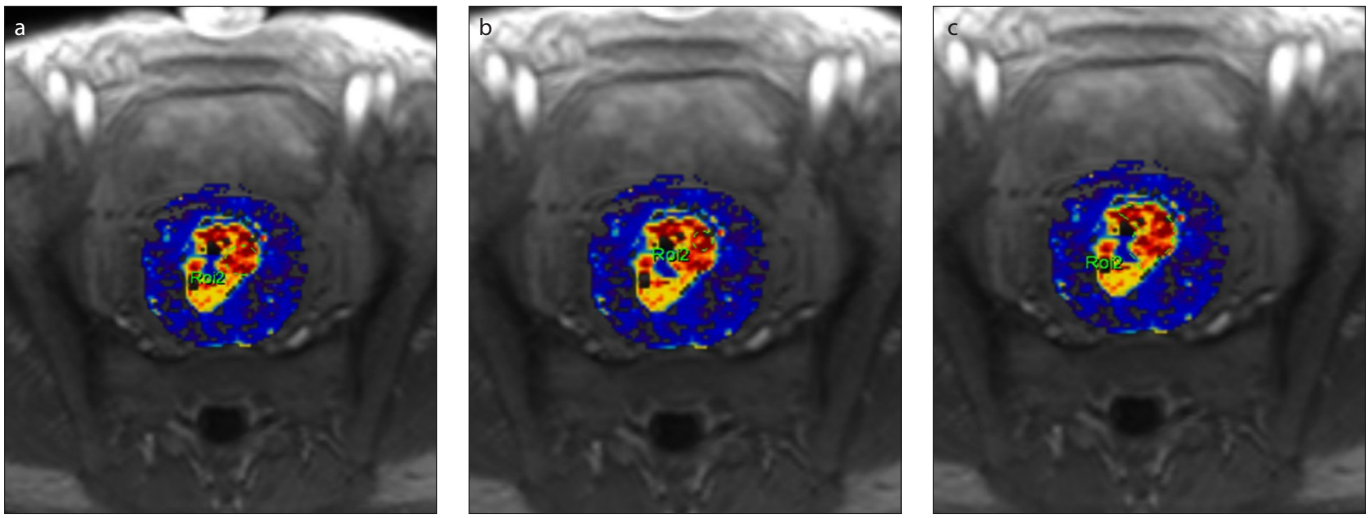

Figure 2. a–c. K_{trans} color coded maps of the tumoral segment in Fig. 1 showing three different techniques of ROI placements.

value, ADC value on the slice showing maximum wall thickening, ADC obtained with freehand ROI containing as much tumor as possible on the slice showing maximum wall thickening, k_{trans} on the slice showing maximum wall thickening, freehand k_{trans} involving as much tumor as possible on the slice showing maximum wall thickening, k_{trans} measured from red spots with maximum deviation from baseline value.

As far as maximum wall thickness was concerned, the mean (median)± standard deviation of the first measurement performed by the first radiologist was 20.80 (19.8)±5.23 mm, and the mean of the second measurement was 20.48 (19.5)±4.61 mm. No statistically significant difference was observed between the two measurements (intraclass correlation coefficient [ICC], 0.987).

Mean length of the involved segment was measured as 56.34(55.4)±13.66 mm and 56.46 (53.8)±13.15 mm by the first radiologist. There was no statistically significant difference between the two measurements (ICC, 0.957).

The mean value of the lowest ADC was measured as 721.31(712.6)±147.18 mm^2/s and 718.96 (707.0)±135.71 mm^2/s by the first radiologist. Statistical analysis showed no significant difference between the two measurements (ICC, 0.982).

The mean value of the ADC measured on the slice with maximum wall thickness was measured as 829.90 (791.5)±144.24 mm^2/s and 829.48(796.9)±149.23 mm^2/s by the first observer. The two measurements did not differ significantly (ICC, 0.985).

The mean of the ADC value measured by freehand ROI on the slice with maximum wall thickness was 846.56(823.0)±136.31 mm^2/s for the first and 848.23(806.4)±144.15 mm^2/s for the second measurement by the first observer. Statistical analysis revealed that they did not differ significantly (ICC, 0.976).

The mean of the k_{trans} value measured on the slice with maximum wall thickness was measured as 0.219 (0.202)±0.080 and 0.214 (0.198)±0.074 by the first radiologist. There was statistically no significant difference among two measurements (ICC, 0.978).

The mean of the k_{trans} measured by freehand ROI technique (including as much tumoral tissue as possible) was 0.208(0.200)±0.074 and 0.207(0.196)±0.069, by the first observer. Statistical analysis showed no significant difference among two different measurements of the first observer (ICC, 0.979).

The mean of the k_{trans} measured from the dark red foci was 0.308(0.280)±0.109 as the first measurement and 0.311(0.302)±0.105 as the second measurement by the first observer. Statistical analysis showed no difference in between (ICC, 0.985).

After intraobserver analysis was completed, interobserver analysis was performed by comparing values measured by three different observers. The mean values of the parameters measured by three different observers and statistical analysis results are given in Table 1.

As far as interobserver variability was considered, only one parameter, the ADC value measured on the slice with maximum wall thickness, differed significantly. As shown in Table 2, there was not statistically significant difference between the readings of the observers regarding the other 7 parameters. For interobserver variability, again, for all the comparisons, Bland Altman confidence interval data was calculated.

Maximum wall thickness values were measured as 20.6 (20.3)±4.8, 20.4 (20.5)±5.2, and 20.5 (20.5)±5.2, by observer 1, 2, and 3, respectively, with no statistically significant difference among the measurements. Bland Altman analysis showed that the values were within the confidence interval.

No statistically significant difference was found among the measurements of the three observers regarding the maximum sagittal length of the tumoral segment, measured as 56.4 (54.3)±13.3, 74.3 (54.5)±94.2 and 74.3 (54.5)±94.2. Bland Altman analysis showed that the values were within the confidence interval.

The mean of the lowest ADC was 720.1 (710.5)±140.8 for the first, 715.1 (713.5)±134.7 for the second and 714.6 (707.9)±140.9 for the third observer. Bland Altman analysis showed that the values were within the confidence interval.

Mean ADC measurement on the same slice with maximum wall thickness was 829.6 (788.3)±145.6 for the first, 813.3 (794.4)±133.9 for the second, and 810.7 (775.2)±140.8 for the third observer. There was statistically significant difference among the values ($P < 0.01$) (Table 2). Bland Altman analysis showed that the values were within the confidence interval.

Similarly, there was no statistically significant difference among the freehand ADC values, k_{trans} values on the thickest slice, freehand k_{trans} values, and k_{trans} values obtained for the dark red focus measured by the three observers (Table 2). Bland Altman analysis showed that all values were within the confidence interval.

Table 1. Comparison of different measurements by the first observer

		Wilcoxon test		Bland Altman analysis			
Variables	Obs	Mean (Median)±SD	*P* [a]		Difference	Lower Limit	Upper Limit
Max diameter	Obs1.1	20.80 (19.8)±5.23	0.44	Value (SD)	0.323 (1.99)	-3.59 (0.63)	4.24 (0.63)
	Obs1.2	20.48 (19.5)±4.61		95% CI	-0.42; 1.070	-4.88; -2.30	2.95; 5.53
Sagittal length	Obs1.1	56.34 (55.4)±13.66	0.97	Value (SD)	0.120 (3.03)	-6.07 (0.95)	5.83 (0.95)
	Obs1.2	56.46 (53.8)±13.15		95% CI	-1.25; 1.014	-8.036; -4.11	3.88; 7.79
Lowest ADC	Obs1.1	721.31 (712.6)±147.18	0.47	Value (SD)	2.35 (30.23)	-56.90 (9.54)	61.62 (9.54)
	Obs1.2	718.96 (707.0)±135.71		95% CI	-8.93; 13.64	-76.42; -37.39	42.10; 81.13
Same slice ADC	Obs1.1	829.90 (791.5)±144.24	0.81	Value (SD)	0.41 (35.60)	-69.37 (11.23)	70.20 (11.23)
	Obs1.2	829.48 (796.9)±149.23		95% CI	-12.87; 13.71	-92.34; -46.39	47.22; 93.18
Freehand ADC	Obs1.1	846.56 (823.0)±136.31	0.97	Value (SD)	-1.67 (43.03)	-86.01 (13.57)	82.66 (13.57)
	Obs1.2	848.23 (806.4)±144.15		95% CI	-17.74; 14.39	-113.7; -58.24	54.89; 110.43
Thickest slice k_{trans}	Obs1.1	0.219 (0.202)±0.080	0.16	Value (SD)	0.004 (0.022) 80.0229	-0.039 (0.007)	0.04 (0.007)
	Obs1.2	0.214 (0.198)±0.074		95% CI	-0.0036; 0.013	-0.054; -0.025	0.034; 0.064
Freehand k_{trans}	Obs1.1	0.208 (0.200)±0.074	0.81	Value (SD)	0.001 (0.002)	-0.039 (0.006)	0.004 (0.006)
	Obs1.2	0.207 (0.196)±0.069		95% CI	-0.006; 0.008	-0.053; -0.02	0.028; 0.055
Dark red k_{trans}	Obs1.1	0.308 (0.280)±0.109	0.39	Value (SD)	-0.004 (0.03)	-0.06 (0.009)	0.055 (0.009)
	Obs1.2	0.311 (0.302)±0.105		95% CI	-0.015; 0.007	-0.08; -0.04	0.003; 0.074

Bland Altman Analysis : One row per subject with only one replicate for each method.
CI, confidence interval; SD, standard deviation; Obs, observer.
[a]Wilcoxon test *P* value.

In comparison of the ADC values obtained from the slice with maximum wall thickness, there was significant difference among the three observers using the Wilcoxon test. The values are given in Table 3. Although there was significant difference for this parameter in Wilcoxon test, we think that the results of Bland Altman test are more valid for this analysis. For this parameter Bland Altman analysis revealed that only 2 points were outside the confidence interval for the first and second observers, 2 points for the first and third observers, and 3 points for the second and third observers.

Discussion

Multiparametric MRI of the rectum includes diffusion-weighted sequence and perfusion study, in addition to routine sequences. Diffusion-weighted images are acquired by applying magnetic gradients in several directions and supplies data about Brownian motion, which is the random motion of water molecules in tissues (4). By the help of DWI, it is possible to quantify Brownian motion in various tissues, in the form of ADC. It is well known that a number of pathological conditions including tumorigenesis creates obstacles to the diffusion of water molecules in tissues. These obstacles may be due to increased cellularity, increased cell membrane, protein or macromolecule content (19). Hence, DWI provides quantitative data about cellular changes at the molecular level. There are a number of important technical parameters related with DWI. One of the most important advances in DWI, is small FOV DWI sequence. Conventional DWI sequence has important limitations and artifacts that decrease the resolution. The combination of reduced FOV and single-shot echo-planar-imaging (EPI) in the phase encoding direction spatially selective pulses enable decreased acquisition steps and lower EPI echo train. This technique enables receiving high signal from only the area of interest with better resolution without a significant increase in scan time (22, 23). There are only a few studies regarding the utility of small FOV DWI in the literature. In the field of abdominal radiology, small FOV DWI literature includes the pancreas, cervix, testes, prostate, and kidney (24, 25). As far as we could review, there is no feasibility or utility study with small FOV DWI of the rectum in the literature. The current study is performed using the small FOV DWI sequence. In this study, there was no statistically significant difference among the two different ADC measurements performed by the same observer. On the other hand, there was a statistically significant difference for ADC measurements that were performed with circular ROI containing at least 8 pixels performed on the slice with maximum wall thickness. We believe this might have resulted from inadequate number of pixels and tumoral heterogeneity. The lowest ADC values and the ADC measured with freehand ROI containing as much tumor tissue as possible did not differ significantly. This finding shows that small FOV DWI is a reliable technique that can be reproduced choosing the lowest ADC foci or using freehand ROI including as much tumoral tissue as possible. Although previous data regarding DWI of rectal cancer in the literature contain standard FOV DWI technique, their results are mostly similar with our study, regarding feasibility and reproducibility. In 2014, Attenberger et al. (9) performed multiparametric MRI of the rectum containing 54 patients with rectal carcinoma. In addition to treatment response, they evaluated interobserver variability. They performed ADC measurements of the tumor by two

Table 2. Comparison of measurements performed by different observers

Friedman ANOVA				Bland Altman analysis				
Variables	Obs	Mean (median)±SD	*P* [a]	Obs		Difference	Lower limit	Upper limit
Max diameter	Obs1	20.6 (20.3)±4.8	0.59	Obs1	Value (SD)	0.23 (3.25)	-6.1 (1.02)	6.6 (1.02)
				Obs2	95% CI	-0.98; 1.45	-8.25; -4.04	4.52; 8.72
	Obs2	20.4 (20.5)±5.2		Obs1	Value (SD)	0.213 (2.4)	-4.5 (0.76)	4.9 (0.76)
				Obs3	95% CI	-0.68; 1.11	-6.06; -2.95	3.38; 6.49
	Obs3	20.5 (20.5)±5.2		Obs2	Value (SD)	-0.02 (2.04)	-4.04 (0.6)	3.9 (0.64)
				Obs3	95% CI	-0.78; 0.74	-5.36; -2.71	2.67; 5.31
Sagittal length	Obs1	56.4 (54.3)±13.3	0.67	Obs1	Value (SD)	-0.80 (6.07)	-12 (1.91)	11.10 (1.91)
				Obs2	95% CI	-3.07; 1.46	-16.64; -8.79	7.18; 15.02
	Obs2	74.3 (54.5)±94.2		Obs1	Value (SD)	-0.21 (3.44)	-6.9 (1.08)	6.53 (1.08)
				Obs3	95% CI	-1.49; 1.07	-9.17; -4.73	4.31; 8.75
	Obs3	56.6 (54.5)±11.8		Obs2	Value (SD)	0.59 (4.29)	-7.83 (1.35)	9.02 (1.35)
				Obs3	95% CI	-1.008; 2.20	-10.60; -5.05	6.24; 11.79
Lowest ADC	Obs1	720.1 (710.5)±140.8	0.10	Obs1	Value (SD)	5.05 (25.22)	-44.39 (7.96)	54.4 (7.96)
				Obs2	95% CI	-4.37; 14.47	-60.68; -28.11	38.21; 70.78
	Obs2	715.1 (713.5)±134.7		Obs1	Value (SD)	5.55 (18.20)	-30.12 (5.74)	41.23 (5.74)
				Obs3	95% CI	-1.24; 12.35	-41.8; -18.37	29.48; 52.9
	Obs3	714.6 (707.9)±140.9		Obs2	Value (SD)	0.50 (16.74)	-32.31 (5.2)	33.3 (5.2)
				Obs3	95% CI	-5.74; 6.75	-43.1; -21.5	22.5; 44.13
Same slice ADC	Obs1	829.6 (788.3)± 145.6	<0.001	Obs1	Value (SD)	16.30 (36.3)	-55.8 (11.6)	88.4 (11.6)
				Obs2	95% CI	2.55; 30.04	-79.6; -32.09	64.6; 112.2
	Obs2	813.3 (794.4)± 133.9		Obs1	Value (SD)	18.9 (25.4)	-30.8 (8.01)	68.7 (8.01)
				Obs3	95% CI	9.49; 28.47	-47.1; -14.4	52.37; 55.1
	Obs3	810.7 (775.2)±140.8		Obs2	Value (SD)	2.68 (24.4)	-45.27 (7.7)	50.64 (7.7)
				Obs3	95% CI	-6.45; 11.82	-61.07; -29.4	34.8; 66.43
Freehand ADC	Obs1	847.3 (815.8)±138.6	0.67	Obs1	Value (SD)	-7.79 (32.3)	-71.22 (10.2)	55.63 (10.2)
				Obs2	95% CI	-19.8; 4.28	-92.11; -50.34	34.7; 76.5
	Obs2	855.1 (820.0)±145.9		Obs1	Value (SD)	-1.53 (34.5)	-69.3 (10.9)	66.2 (10.9)
				Obs3	95% CI	-14.45; 11.3	-91.6; -47.01	43.9; 88.5
	Obs3	848.9 (812.5)±141.3		Obs2	Value (SD)	6.26 (46.2)	-84.3 (14.5)	96.8 (14.5)
				Obs3	95% CI	-11.0; 23.52	-114.2; -54.5	67.0; 126.7
Thickest slice k_{trans}	Obs1	0.217 (0.201)±0.077	0.97	Obs1	Value (SD)	0.002 (0.02)	-0.038 (0.006)	0.04 (0.006)
				Obs2	95% CI	-0.004; 0.001	-0.05; -0.02	0.03; 0.05
	Obs2	0.214 (0.202)±0.067		Obs1	Value (SD)	0.004 (0.01)	-0.02 (0.005)	0.03 (0.005)
				Obs3	95% CI	-0.002; 0.01	-0.03; -0.017	0.025; 0.04
	Obs3	0.213 (0.198)±0.069		Obs2	Value (SD)	0.01 (0.01)	-0.02 (0.003)	0.02 (0.003)
				Obs3	95% CI	-0.003; 0.005	-0.03; -0.01	0.01; 0.03
Freehand k_{trans}	Obs1	0.208 (0.199)±0.071	0.072	Obs1	Value (SD)	-0.003 (0.034)	-0.07 (0.010)	0.06 (0.01)
				Obs2	95% CI	-0.01; 0.009	-0.094; -0.04	0.041; 0.086
	Obs2	0.212 (0.201)±0.069		Obs1	Value (SD)	0.002 (0.030)	-0.07 (0.01)	0.07 (0.01)
				Obs3	95% CI	-0.01; 0.016	-0.09; -0.046	0.05; 0.10
	Obs3	0.205 (0.197)±0.071		Obs2	Value (SD)	0.006 (0.01)	-0.02 (0.005)	0.04 (0.005)
				Obs3	95% CI	-0.0001; 0.01	-0.039; -0.01	0.02; 0.05

Table 2. Comparison of measurements performed by different observers (cont'd)

	Friedman ANOVA			Bland Altman analysis				
Variables	Obs	Mean (median)±SD	*P* [a]	Obs		Difference	Lower limit	Upper limit
Dark red k_{trans}	Obs1	0.310 (0.298)±0.107	0.39	Obs1	Value (SD)	0.0001 (0.02)	-0.05 (0.008)	0.05 (0.008)
				Obs2	95% CI	-0.01; 0.010	-0.007; -0.035	0.036; 0.071
	Obs2	0.309 (0.308)±0.103		Obs1	Value (SD)	0.003 (0.026)	-0.04 (0.008)	0.05 (0.008)
				Obs3	95% CI	-0.006; 0.012	-0.065; -0.03	0.037; 0.007
	Obs3	0.307 (0.280)±0.106		Obs2	Value (SD)	0.002 (0.018)	-0.03 (0.005)	0.03 (0.005)
				Obs3	95% CI	-0.004; 0.009	-0.04; -0.021	0.02; 0.051

Bland Altman analysis: One row per subject with only one replicate for each method.
CI, confidence interval; SD, standard deviation; Obs, observer.
[a]Friedman ANOVA test *P* value.

Table 3. Statistical analysis of the same slice ADC parameter among observers

Variables		Mean (median)±SD	*P* [a]
Same slice ADC	Obs1	829.693 (788.39)±145.676	<0.05
	Obs2	813.392 (794.45)±133.994	
Same slice ADC	Obs1	829.693 (788.39)±145.676	<0.001
	Obs3	810.708 (775.28)±140.899	
Same slice ADC	Obs2	813.392 (794.45)±133.994	0.32
	Obs3	810.708 (775.28)±140.899	

ADC, apparent diffusion coefficient; SD, standard deviation; Obs, observer.
[a]Wilcoxon test *P* value.

different observers. They found that interreader correlation was good to very good for ADC of the tumoral tissue. ADC measurements in their study has been performed with a single technique, different from ours (9). In 2016, Hotker et al. (12) performed a retrospective study including 24 patients with rectal carcinoma to investigate the role of multiparametric MRI in the evaluation of treatment response. In their study, they also evaluated interreader variability, using DWI volumetry. They determined that interreader agreement differed greatly among DWI measurements with better agreement on pretreatment compared with post-treatment values. Their results were different from the previous study by Attenberger et al. (9) and our study, possibly due to different technical parameters and measurement techniques. In 2017, Attenberger et al. (24) published a second article about multiparametric rectum MRI that also included feasibility. They performed DWI in a total of 21 patients for rectal carcinoma, and found good interobserver variability, as far as ADC values are concerned. Another study regarding feasibility was performed by Sun et al. (25), including 52 patients with rectal adenocarcinoma. They observed excellent interreader correlation for ADC measurements of tumoral tissue, similar to our study.

The other component of multiparametric rectal MRI is perfusion imaging. Perfusion imaging provides data about the local microcirculation and capillary permeability of the tumor by measuring changes in signal intensity over time (4). It is performed by using a paramagnetic contrast agent and acquiring a T1-weighted sequence with a high temporal resolution. Changes in signal intensity over time are then evaluated in a semiquantitative or quantitative way, using a number of pharmacokinetic models (Tofts, Tofts and Kermode, and Brix et al) (4). K_{trans}, the perfusion parameter used in this study, is a quantitative parameter derived from perfusion imaging that pertains to the contrast agent transfer rate between blood and tissue. Our study showed that k_{trans} measurements can be repeated with high accuracy among observers for all the three measurement techniques used. Attenberger et al. (9), in the feasibility part of their multiparametric rectal MRI study, used a different parameter from our study for perfusion imaging, which is plasma flow. They found good interreader correlation for this parameter. But, since the parameters are different, it is not possible to compare our results with the results of their study. In another study using DCE volumetry, Hötker et al. (12) reported significant interobserver variability among the perfusion parameters. Their perfusion parameters were k_{trans} and DCE-volumetry. Their results are different from our study, possibly due to different technical parameters and measurement techniques. Sun et al. (25) performed another feasibility study where they used intravoxel incoherent motion (IVIM) technique and hence different parameters for perfusion. Their perfusion parameters were pseudodiffusion coefficient and perfusion fraction, which yielded excellent interobserver agreement.

There are three limitations of this study: we had a limited number of patients; the study was retrospective in nature; and volumetric assessment was not perfomed since we did not have the required software. Also, an important limitation for perfusion and diffusion imaging of the rectum is the lack of standardization as far as hardware, software and measurement techniques are concerned. This impedes comparability of different studies.

In conclusion, we used three different measurement techniques for each modality and found good to excellent intra and interobserver agreement, except for a single measurement technique. This study shows the repeatability of ADC and k_{trans} measurements obtained from multiparametric rectum imaging. At present, multiparametric MRI of the rectum is an experimental technique, but it is emerging as a promising tool. To understand the role of multiparametric imaging in prediction of treatment response and evaluation of neoadjuvant

treatment response, future studies with larger patient groups are needed to be analyzed, in order to validate the role of this technique.

Conflict of interest disclosure

The authors declared no conflicts of interest.

References

1. Blazic IM, Campbell NM, Gollub MJ. MRI for evaluation of treatment response in rectal cancer. Br J Radiol 2016; 89:20150964. [CrossRef]
2. Balyasnikova S, Brown G. Imaging advances in colorectal cancer. Curr Colorectal Cancer Rep 2016; 12:162–169. [CrossRef]
3. Jhaveri KS, Hosseini-Nik H. MRI of rectal cancer: an overview and update on recent advances. AJR Am J Roentgenol 2015; 205:W42–55. [CrossRef]
4. Hötker AM, Garcia-Aguilar J, Gollub MJ. Multiparametric MRI of rectal cancer in the assessment of response to therapy: a systematic review. Dis Colon Rectum 2014; 57:790–799. [CrossRef]
5. Pham TT, Liney G, Wong K, et al. Study protocol: multi-parametric magnetic resonance imaging for therapeutic response prediction in rectal cancer. BMC Cancer 2017; 17:465. [CrossRef]
6. Park MJ, Kim SH, Lee SJ, Jang KM, Rhim H. Locally advanced rectal cancer: added value of diffusion-weighted MR imaging for predicting tumor clearance of the mesorectal fascia after neoadjuvant chemotherapy and radiation therapy. Radiology 2011; 260:771–780. [CrossRef]
7. Engin G, Sharifov R, Güral Z, et al. Can diffusion-weighted MRI determine complete responders after neoadjuvant chemoradiation for locally advanced rectal cancer? Diagn Interv Radiol 2012; 18:574–581. [CrossRef]
8. Balyasnikova S, Brown G. Optimal imaging strategies for rectal cancer staging and ongoing management. Curr Treat Options Oncol 2016; 17:32. [CrossRef]
9. Attenberger UI, Pilz LR, Morelli JN, et al. Multi-parametric MRI of rectal cancer - do quantitative functional MR measurements correlate with radiologic and pathologic tumor stages? Eur J Radiol 2014; 83:1036–1043. [CrossRef]
10. Lambregts DMJ, Delli Pizzi A, Lahaye MJ, et al. A pattern-based approach combining tumor morphology on MRI with distinct patterns on diffusion-weighted imaging to assess response of rectal tumors after chemoradiotherapy. Dis Colon Rectum 2018; 61:328–337. [CrossRef]
11. Delli Pizzi A, Cianci R, Genovesi D, et al. Performance of diffusion-weighted magnetic resonance imaging at 3.0 T for early assessment of tumor response in locally advanced rectal cancer treated with preoperative chemoradiation therapy. Abdom Radiol 2018; 43:2221–2230. [CrossRef]
12. Hötker AM, Tarlinton L, Mazaheri Y, et al. Multiparametric MRI in the assessment of response of rectal cancer to neoadjuvant chemoradiotherapy: A comparison of morphological, volumetric and functional MRI parameters. Eur Radiol 2016; 26:4303–4312. [CrossRef]
13. Gürses B, Böge M, Altınmakas E, Balık E. Multiparametric MRI in rectal cancer. Diagn Interv Radiol 2019; 25:175–182. [CrossRef]
14. Beets-Tan RGH, Lambregts DMJ, Maas M, et al. Magnetic resonance imaging for clinical management of rectal cancer: Updated recommendations from the 2016 European Society of Gastrointestinal and Abdominal Radiology (ESGAR) consensus meeting. Eur Radiol 2018; 28:1465–1475. [CrossRef]
15. Delli Pizzi A, Basilico R, Cianci R, et al. Rectal cancer MRI: protocols, signs and future perspectives radiologists should considering everyday clinical practice. Insights Imaging 2018; 9:405–412. [CrossRef]
16. Yeo DM, Oh SN, Jung CK, et al. Correlation of dynamic contrast-enhanced MRI perfusion parameters with angiogenesis and biologic aggressiveness of rectal cancer: Preliminary results. J Magn Reson Imaging 2015; 41:474–480. [CrossRef]
17. Martens MH, Subhani S, Heijnen LA, et al. Can perfusion MRI predict response to preoperative treatment in rectal cancer? Radiother Oncol 2015; 114:218–223. [CrossRef]
18. Hötker AM, Tarlinton L, Mazaheri Y, et al. Multiparametric MRI in the assessment of response of rectal cancer to neoadjuvant chemoradiotherapy: A comparison of morphological, volumetric and functional MRI parameters. Eur Radiol 2016; 26:4303–4312. [CrossRef]
19. Lambregts DM, Beets GL, Maas M, et al. Tumour ADC measurements in rectal cancer: effect of ROI methods on ADC values and interobserver variability. Eur Radiol 2011; 21:2567–2574. [CrossRef]
20. Blazic IM, Lilic GB, Gajic MM. Quantitative assessment of rectal cancer response in neoadjuvant combined chemotherapy and radiation therapy: Comparison of three methods of positioning of region of interest for ADC measurements at diffusion-weighted imaging. Radiology 2017; 282:615. [CrossRef]
21. Nguyen TL, Soyer P, Fornès P, Rousset P, Kianmanesh R, Hoeffel C. Diffusion-weighted MR imaging of the rectum: clinical applications. Crit Rev Oncol Hematol 2014; 92:279–295. [CrossRef]
22. Riffel P, Michaely HJ, Morelli JN, et al. Zoomed EPI-DWI of the pancreas using two-dimensional spatially-selective radiofrequency excitation pulses. PLoS One 2014; 9:e89468. [CrossRef]
23. Yıldırım İO, Sağlık S, Çelik H. Conventional and ZOOMit DWI for evaluation of testis in patients with ipsilateral varicocele. AJR Am J Roentgenol 2017; 208:1045–1050. [CrossRef]
24. Attenberger UI, Ong MM, Rathmann N, et al. mMRI at 3.0 T as an evaluation tool of therapeutic response to neoadjuvant CRT in patients with advanced-stage rectal cancer. Anticancer Res 2017; 37:215–222. [CrossRef]
25. Sun H, Xu Y, Song A, Shi K, Wang W. Intravoxel incoherent motion MRI of rectal cancer: correlation of diffusion and perfusion characteristics with prognostic tumor markers. AJR Am J Roentgenol 2018; 210:W139–W147. [CrossRef]